DESIGN AND SYNTHESIS OF BIOCOMPATIBLE MAGNETIC FERRITE NANOPARTICLES CONJUGATED WITH ANGIOPEP FOR LRP-1 RECEPTOR-MEDIATED DELIVERY

[1]Seipati MOKHOSI, [2]Wendy MDLALOSE, [1]Moganavelli SINGH

[1]Discipline of Biochemistry, University of Kwazulu-Natal, Westville Campus, Republic of South Africa, MokhosiS@ukzn.ac.za

[2]Discipline of Physics, University of Kwazulu-Natal, Westville Campus, Republic of South Africa, MdlaloseW@ukzn.ac.za

https://doi.org/10.37904/nanocon.2023.4758

Abstract

Disorders and diseases of the brain present an enormous challenge due to the physical and physiological properties of the blood-brain barrier (BBB), making entry for therapeutics difficult. In recent years, increased research has focused on using magnetic ferrite nanoparticles (NPs) in various biomedical applications. In this study, we report on the design of ferrite NPs for traversing the BBB. Core ferrite $CoFe_2O_4$ and $Mg_{0.5}Co_{0.5}Fe_2O_4$ NPs were synthesized using the glycol-thermal route and coated with chitosan (CS). A BBB-targeting peptide, Angiopep-2 (ANG), was covalently conjugated to the coated NPs. The physical, chemical, and magnetic properties of the core and derivative ferrite NPs were characterized by X-ray diffraction (XRD), Fourier transform infrared spectroscopy (FTIR), high-resolution transmission electron microscopy (HR-TEM), nanoparticle tracking analysis (NTA) and vibrating sample magnetometer (VSM). Docking studies were conducted using Autodock Vina software for binding. XRD, HR-TEM and VSM results revealed spinel crystalline ferrite core NPs exhibiting superparamagnetic behaviour. Particle core sizes of the ferrite NPs were below 13.6 nm. The FTIR spectra showed characteristic peak shifts upon CS-coating and conjugation with Angiopep-2, thus confirming functionalization. Hydrodynamic sizes of 90.4 nm and 152. nm were reported for the ANG-CS-$CoFe_2O_4$, and ANG-CS-$Mg_{0.5}Co_{0.5}Fe_2O_4$, respectively. ANG-CS-$Mg_{0.5}Co_{0.5}Fe_2O_4$ presented the most stability with a zeta potential (+29.0 mV), while ANG-CS-$CoFe_2O_4$ has +19.2 mV. Molecular docking investigations revealed binding energies for the CS-conjugated ANG of -5.67 kCal/mol, suggesting that the LRP-1 receptor was not significantly hindered. These NPs exhibit potential for targeted CNS delivery and can be explored for *in vitro* gene and drug delivery.

Keywords: Ferrites, magnetic nanoparticles, Angiopep, blood-brain barrier, docking, LRP-1 receptor

1. INTRODUCTION

Disorders and diseases of the central nervous system present an enormous challenge, primarily due to the tight blood-brain barrier (BBB), an essential membrane component in the brain [1]–[3]. The BBB comprises specialized endothelium of the brain micro-vessels that restrict the influx of certain compounds, including drugs, while allowing for the entry of nutrients [4]. Therapeutic access is thus tricky and has forced researchers to explore approaches other than traditional radiation, chemotherapy, and surgery. These are often invasive and ineffective, leading to unwanted side effects [5].

Nanotechnology entails the design of suitable nanoparticles (NPs) as carriers of therapeutics, particularly critical in CNS-targeted therapy, where size is a limiting factor in traversing the BBB [6]. Ferrites (denoted with formula MFe_2O_4) have emerged as attractive iron oxide-based magnetic NPs with reports on their use in drug delivery [7]–[9]. This is due to their unique properties, such as metal substitution in synthesis design, high magnetization saturation, and easy surface functionalization [8], [10]. However, magnetic NPs present inherent

tendencies to aggregate, which results in short-term stability in biological suspensions [11]–[13]. Hence, modifications of the NPs using polymers such as polyethylene glycol (PEG) and chitosan (CS) often resolve these challenges[14]. Recently, there have been reports on the synthesis of biocompatible and stable polymer-coated magnesium-doped ferrite derivatives using PEG, PVA, and chitosan, and showed their potential in the delivery of the anti-cancer drugs, doxorubicin and 5-fluorouracil [15]–[17].

The low-density lipoprotein receptor-related protein (LRP-1) is a 600 kDa receptor ubiquitously expressed in the brain [18]. Thus, this receptor presents an essential highway for transport across the BBB. Angiopep-2 is a widely studied ligand for receptor-mediated transcytosis via the LRP-1 receptor[19]–[21]. A recently FDA-approved novel ANG1005, comprising 3 paclitaxel molecules covalently linked to Angiopep-2, was shown to bind to the low-density LRP-1 to treat glioblastoma multiforme [22], [23].

In this study, we designed and synthesized biocompatible ferrite NPs ($CoFe_2O_4$ and $Mg_{0.5}Co_{0.5}Fe_2O_4$) for LRP-1-targeted delivery. The synthesized NPs were coated with CS using sodium tripolyphosphate (TPP) as a crosslinker. After that, a cysteine-modified Angiopep-2 (AngiopepC) was covalently conjugated to the NPs. Furthermore, Molecular docking was carried out to explore the potential of the ferrite NPs for LRP-1 binding.

2. MATERIALS AND METHOD

2.1 Raw materials

Cobalt chloride tetrahydrate ($CoCl_2{\cdot}4H_2O$, 98%), iron (III) chloride tetrahydrate ($FeCl_2{\cdot}4H_2O$, 98%), magnesium chloride hexahydrate ($Cl_2Mg{\cdot}6H_2O$, 99%), sodium tripolyphosphate [TPP, 85% (w/w)], and ≥75% deacetylated chitosan from shrimp shells; $(C_6H_{11}NO_4)n$; MWCO 50,000-190,000 Da, was purchased from Sigma-Aldrich, St. Louis, MO, USA. Dimethylformamide (DMF), phosphate-buffered saline tablets (PBS [140 mM NaCl, 10 mM phosphate buffer, 3 mM KCl, ethidium bromide, glacial acetic acid were sourced from Merck (Darmstadt, Germany). Cysteine-modified Angiopep-2 (Angiopep-C) with amino acid chain: TFFYGGSRGKRNNFKTEEY-C was purchased from GenScript Biotech (Netherlands). Chemical reagents of analytical quality were used in this study without any further purification, and ultrapure 18 MΩ Milli-Q water (pH 6.8) was used throughout.

2.2 Synthesis and coating of NPs

$CoFe_2O_4$ and $Mg_{0.5}Co_{0.5}Fe_2O_4$ NPs were produced via a glycol-thermal reaction with the use of stoichiometric measurements of $CoCl_2{\cdot}4H_2O$, $FeCl_2{\cdot}4H_2O$, and $Cl_2Mg{\cdot}6H_2O$, in a protocol by Dlamini *et al*. [24]. The powdered NPs were then coated with CS using a previously reported method with some modifications [25]. Firstly, 0.50 g of CS was dissolved in 100 ml of acetic acid (pH ~ 4) and stirred using the IKA RW 20 Digital Dual-Range Mixer System set at high speed (950 rpm) to produce a chitosan solution. Thereafter, 0.24 g of tri-polyphosphate (TPP) was dissolved in 100 ml of deionized water. This TPP solution was added dropwise to the chitosan solution with stirring. Finally, approximately 0.20 g of the synthesized ferrite NPs were added to the TPP-chitosan mixture with stirring at 450 rpm. The TPP-crosslinked CS-coated MNP mixture was stirred for 20 hours at room temperature. Finally, the NPs were separated from the black homogeneous mixture using an external magnet. After several washes with deionized water, the samples were dried overnight under an infrared lamp. The homogenized powder was obtained using a mortar and pestle.

2.3 Conjugation of CS-NPs with AngiopepC

AngiopeC was conjugated onto the CS-coated ferrite NPs with modifications [26]. Briefly, a stock solution of CS-coated ferrite NPs was prepared in triple distilled water (5 mg/ml). To this was added 0.25 µmole of short-chain crosslinker *N*-succinimidyl-3-(2-pyridithiol) propionate (SPDP) dissolved in dimethylformamide (DMF). The solution was stirred for 2 hours in the dark at room temperature (25 ℃) until the pyridithiol-activated CS-coated NPs formed. An external magnet was then used to separate the unbound SPDP, which was discarded with the supernatant. AngiopepC (0.25 µmoles) was prepared in triple distilled water and added to allow

sulfhydryl conjugation to the NPs. The solution was stirred for an additional 3.5 hours, and the resultant ferrite NPs, *viz*. ANG-CS-$CoFe_2O_4$ and ANG-CS-$Mg_{0.5}Co_{0.5}Fe_2O_4$ were separated using an external magnet. The supernatant was discarded, and the NPs were dried at 30 ℃ and ground to a fine powder using a marble pestle and mortar.

2.4 Characterization of synthesized NPs

Transmission electron microscopy (TEM) measurements were performed on the JEOL JEM-1010 TEM operated at an accelerated voltage of 100 kV. The MegaView III Soft Imaging Systems (SIS), the side-mounted 3-megapixel digital camera, was used to document the micrographs. A Perkin Elmer Spectrum 100 FTIR (Fourier Transform Infrared) spectrometer fitted with a universal attenuated total reflectance (ATR) component was used for the FTIR analyses. The zeta potential measurements and hydrodynamic size distributions were assessed by nanoparticle tracking analysis (NTA) using a NanoSight NS500 and analyzed using the NanoSight NTA version 3.2 software. Magnetic measurements were obtained using a LakeShore Model 735 Vibrating Sample Magnetometer, subjected to an applied magnetic field of 14 kOe. All characterizations were performed at room temperature.

2.5 Molecular docking studies

Computer-guided docking studies were carried out using the AutoDock Vina software. The cysteine-modified Angiopep-2 (AngiopepC) and the CS-coated AngiopepC were adapted using Chemdraw for molecular docking for the LDL receptor (Protein Data Bank ID -1N7D). The X-ray crystal structure of the LDL receptor (1N7D) was downloaded from the Protein Data Bank website (https://www.rcsb.org/) [27]. The active ligands were prepared by hydrogen addition, partial charges calculation, and energy minimization using Force Field MMFF94x. The AutoDock Quick Prep functionality was used for correcting structural issues, 3D protonation, and calculation of partial charges. The Auto Dock Vina protocol detected the best binding poses of the studied ligands, using a triangle matcher as a placement method and London dG as the primary scoring function. The output database comprised the scores of ligand-receptor complexes in kcal/mol. The resulting docking poses were visually examined with BIOVIA Discovery Studio. Only a selection of the best fit into the binding pocket with the top scores for ligand-receptor interactions was made.

3. RESULTS AND DISCUSSION

3.1 Ultrastructural, chemical and magnetic characterization

The XRD spectra of the core $CoFe_2O_4$ and $Mg_{0.5}Co_{0.5}Fe_2O_4$ NPs confirmed single-phase spinel crystalline structures per the JCPDS standard cards no. (JCPDS No. 22–1086), as shown in **Figure 1**. No impurities were observed in the core NPs. The average crystallite size of the uncoated $CoFe_2O_4$ and $Mg_{0.5}Co_{0.5}Fe_2O_4$ was determined to be 9.32 nm and 11.36 nm, respectively. All FTIR spectra shown in **Figure 2** revealed that NPs exhibited the characteristic large peak around 560 cm^{-1}, attributed to the stretching vibrations of Fe^{3+}–O^{2+} complexes at the metal ions' octahedral (B) sites [23]. Functionalization with CS resulted in peak shifts, where a characteristic IR band at 3305 cm^{-1} is due to the O-H bending presenting the absorbed or free water on their surfaces [28]. The peak at 3300 cm^{-1} is assigned to the stretching vibration mode of N−H overlapped with the O–H stretching vibration mode in the ANG-CS-$CoFe_2O_4$ and ANG-CS-$Mg_{0.5}Co_{0.5}Fe_2O_4$. An additional peak observed at 2946 cm^{-1}, characteristic of the C–H stretching, was more pronounced with ANG-conjugation, suggesting an interaction with the peptide. The bands in the 1400 cm^{-1} and 1600 cm^{-1} regions are typically due to the bending vibration of N−H and O−H deformation, respectively. The band at 1628 cm^{-1} is attributed to the C=O of amide group –CONH. The absorption bands at 1200 cm^{-1} and 1300 cm^{-1} were bending vibrations of C–H and C–N, respectively. The peak at 910 cm^{-1} can be assigned to TPP symmetric stretching vibration of the P−O −P bridge [29]

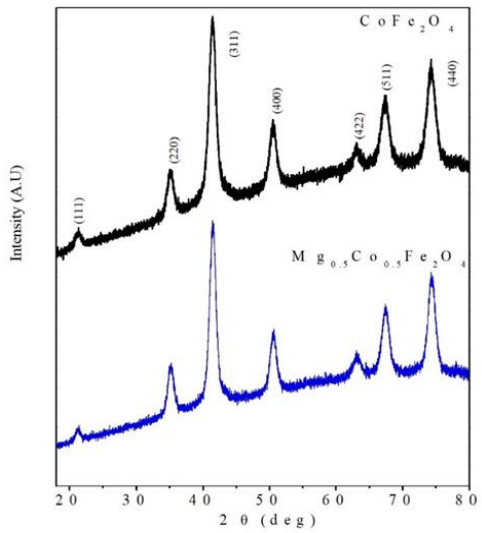

Figure 1 XRD spectra for core $CoFe_2O_4$ and $Mg_{0.5}Co_{0.5}Fe_2O_4$ NPs.

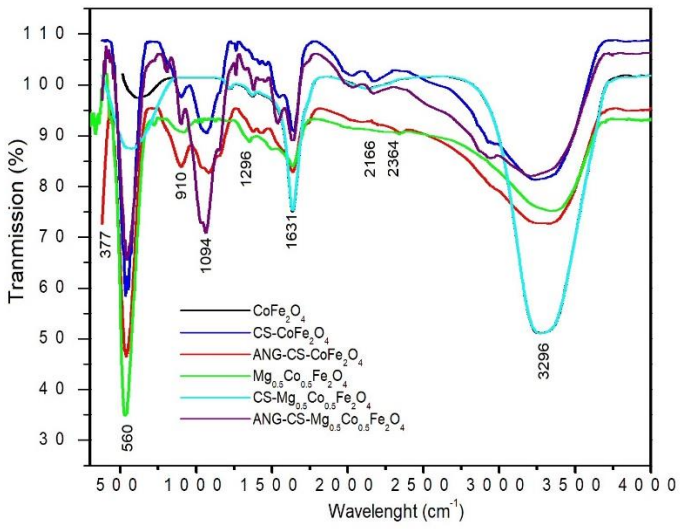

Figure 2 FTIR spectra for $CoFe_2O_4$, CS- $CoFe_2O_4$, ANG-CS-$CoFe_2O_4$, $Mg_{0.5}Co_{0.5}Fe_2O_4$ and CS-$Mg_{0.5}Co_{0.5}Fe_2O_4$ and ANG-CS- $Mg_{0.5}Co_{0.5}Fe_2O_4$

HRTEM analysis in **Figure 3** revealed the uniform spherical morphology of the NPs with no changes after functionalization with chitosan and AngiopepC conjugation. The uncoated CS-$CoFe_2O_4$ NP was 9.32 nm but increased in size upon chitosan functionalization (as shown in **Table 1**). It was consistent with literature, which showed that polymer coating of cobal ferrites could increase the NP sizes [30]. However, while the $Mg_{0.5}Co_{0.5}Fe_2O_4$ recorded a larger value of 13.98 nm, it was compacted to 9.8 nm following CS-coating. A similar trend was observed upon CS-coating of these NPs by adsorption [16]. In both CS-coated ferrite NPs, conjugation with AngiopepC resulted in further size reduction.

NTA results are important in determining the NP sizes in a colloidal suspension. These sizes become more significant than the dry HRTEM sizes, indicating a more realistic sizing in the physiological aqueous environment. The core NPs were the smallest at 86.2 nm for $Mg_{0.5}Co_{0.5}Fe_2O_4$, while the largest diameter was observed in the CS-coated $CoFe_2O_4$ (as presented in **Table 1**). Functionalization with chitosan increased in size, as noted in various reports in the literature, and was attributed to swelling of the chitosan coating [21]. The increase in size was observed to be highest for the $CoFe_2O_4$. Upon conjugation with ANG, a reduction in sizes was observed for both NPs, with drops of 90.4 nm and 152.5 nm noted for ANG-CS-$CoFe_2O_4$ and ANG-CS-$Mg_{0.5}Co_{0.5}Fe_2O_4$ ferrite NPs, respectively. For LRP1-mediated transcytosis in CNS diseases, NPs in the range of 100–200 nm in size are suitable for optimal uptake in the brain [31].The uptake threshold of small particles have to be <200 nm [2], [18], [32].

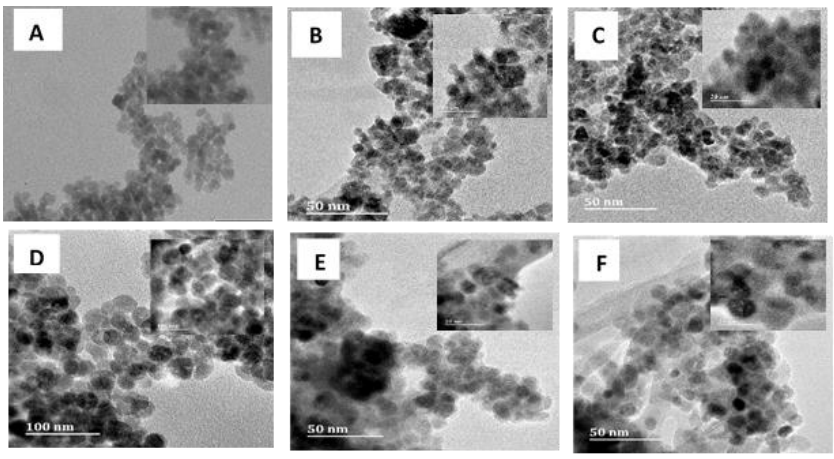

Figure 3 HR-TEM micrographs for (**A**) $CoFe_2O_4$, (**B**) CS-$CoFe_2O_4$, (**C**) ANG-CS-$CoFe_2O_4$, (**D**) $Mg_{0.5}Co_{0.5}Fe_2O_4$, (**E**) CS-$Mg_{0.5}Co_{0.5}Fe_2O_4$, and (**F**) ANG-CS- $Mg_{0.5}Co_{0.5}Fe_2O_4$NPs

Table 1 NP size diameter, hydrodynamic size and zeta potential measurements

	HRTEM	Hydrodynamic Size	Zeta Potential
$CoFe_2O_4$	9.32 nm	86.2 ± 29.5 nm	-1.5 ± 0.3 mV
$Mg_{0.5}Co_{0.5}Fe_2O_4$	12.98 nm	64.9 ± 49.9 nm	1.3 ± 1.2 mV
CS-$CoFe_2O_4$	13.59 nm	240.7 ± 5.4 nm	1.9 ± 0.1 mV
CS-$Mg_{0.5}Co_{0.5}Fe_2O_4$	9.8 nm	161 ± 52.5 nm	20.7 ± 3.2 mV
ANG-CS-$CoFe_2O_4$	8.7 nm	90.4 ± 5.4 nm	19.2 ± 1.3 mV
ANG-CS-$Mg_{0.5}Co_{0.5}Fe_2O_4$	9.5 nm	152.6 ± 13.8 nm	29.0 ± 1.3 mV

Zeta potential magnitude is a good indicator of repulsive forces or charges between particles in suspension. The core ferrite NPs presented the least stability with near-neutral zeta potential measurements. Coating with chitosan significantly improved the stability of the $Mg_{0.5}Co_{0.5}Fe_2O_4$ ferrite NPs, but not the $CoFe_2O_4$ NPs. This indicates that the Co ferrite NPs may still tend to agglomerate more, even after the CS-coating. Interestingly, both derivatives presented better stability following conjugation with Angiopep. A favourable zeta potential of +29.0 mV for ANG-CS-$Mg_{0.5}Co_{0.5}Fe_2O_4$ was noted.

The magnetic properties of the core and CS-coated NPs were studied via VSM, as shown in **Figure 4**. The hysteresis loop of the core NPs core exhibited superparamagnetic behaviour with negligible remanence and coercivity.

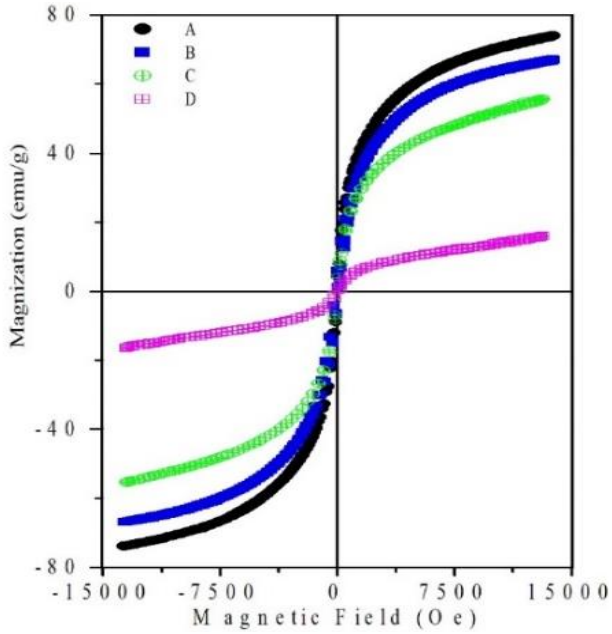

Figure 4 Hysteresis loops for (**A**) $CoFe_2O_4$, (**B**) CS-$CoFe_2O_4$, (**C**) $Mg_{0.5}Co_{0.5}Fe_2O_4$ and (**D**) CS-$Mg_{0.5}Co_{0.5}Fe_2O_4$, NPs.

The highest saturation magnetization (*Ms*) of 73.866 emu/g was reported for the core $CoFe_2O_4$, while $Mg_{0.5}Co_{0.5}Fe_2O_4$ NPs was recorded at 66.89 emu/g. Upon functionalization with TPP-linked CS, a drastic reduction of 16.23 emu/g was noted for $Mg_{0.5}Co_{0.5}Fe_2O_4$, and 59.633 emu/g for $CoFe_2O_4$. Reductions in *Ms* were attributed to the shielding effect of the polymer [17], [33]. TPP-crosslinking of CS added to the shielding of the NPs surface, which has led to further *Ms* reduction when compared to CS coating by adsorption.

3.2. Docking studies

The LRP-1 receptor has been reported to contain 4 clusters of complement-type repeats (CR), with clusters II and III being mainly responsible for ligand binding[34]. The CR56 and CR17 are interesting and have been

linked with the LRP-1 receptor binding [34], [35]. The poses that fit into the binding pocket with top scores and exhibited useful ligand-receptor interactions were selected, as seen in **Figure 5**.

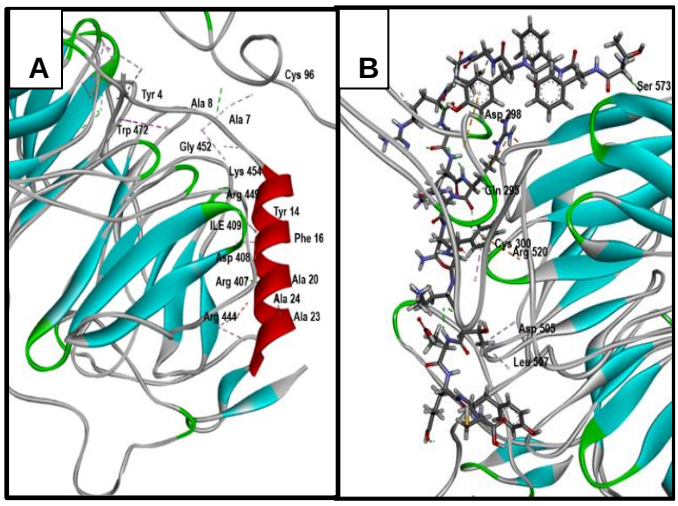

Figure 5 Best docking pose for (**A**) AngiopepC, and (**B**) CS-AngiopepC using Autodock Vina software.

The CS-conjugated AngiopepC presented fewer amino acids interactions, with the characteristic ASP interactions still presented for the CR56 cluster binding (**Table 2**). From the findings of this study and those presented by di Polidoro *et al*, it is believed that the CR56 cluster is most likely involved in the ligand amino acid interactions with the receptor [35].

Table 2 Binding affinity score, and amino acid residues involved in the binding of the free Angiopep and CS-conjugated AngiopepC to LRP-1 receptor

	Binding Affinity (kCal/mol)	**Pi interaction**
AngiopepC	-5.67	**Tyr4, Tyr14, Cys96,** Ala7, Ala8, Ala20, Ala23, Ala24, **Cys96, Arg407, Arg444, Arg449, Asp408, Ile409, Gly452, Lys454,** Trp472
CS-AngiopepC	-5.56	**Cys300, Arg520, Asp298, Asp505, Leu537, Gln295, Ser573**

While the free AngiopepC presented an array of amino acid interactions which have been associated with CR56 cluster binding site *i.e.* CYS, ASP and ARG, additional TYR, PHE, ILE, LYS and GLY have been linked to CR17 cluster [35]. Binding affinities for the free AngiopeC and CS-conjugated AngiopepC were calculated at -5.67 and -5.56 kCal/mol, respectively. It has been previously reported that the acidic residue 959Asp in the CR56 domain binds to the receptor-associated protein (RAP) and is involved in transport across the receptor [35]. From our findings, the AngiopepC/LRP-1 receptor binding would likely mimic the interaction with the RAP protein, where transcytosis would be the most viable means of entry through the LRP-1 receptor. Despite the marginally reduced binding affinity in the CS-conjugated AngiopeC, this would still be the primary form uptake and delivery across the BBB.

4. CONCLUSION

This study achieved successful design and synthesis of derivatives of cobalt ferrite NP. The small-sized and spherically-shaped ferrite NPs exhibited enhanced colloidal stability upon conjugation with the BBB-targeting peptide Angiopep. Docking studies presented a valuable tool in predicting the the affinitiy of the Angiopep conjugated NPs to the receptor. However, further *in vitro* studies should be undertaken to explore the mechanisms of cellular uptake and their potential application for gene delivery. These ferrite NPs demonstrate great potential for LRP-1 receptor-mediated transcytosis in treating CNS disorders and cancers.

REFERENCES

[1] W. M. PARDRIDGE. Drug transport across the blood-brain barrier. *J. Cereb. Blood Flow Metab.* 2012, vol. 32, no. 11, pp. 1959–1972. Available from: https://doi.org/10.1038/jcbfm.2012.126.

[2] S. WOHLFART, S. GELPERINA, and J. KREUTER. Transport of drugs across the blood-brain barrier by nanoparticles. *J. Control. Release*. 2012, vol. 161, no. 2, pp. 264–273. Available from: https://doi.org/10.1016/j.jconrel.2011.08.017.

[3] J. KREUTER. Drug delivery to the central nervous system by polymeric nanoparticles: What do we know?. *Advanced Drug Delivery Reviews*. 2014, vol. 71. Available from: https://doi.org/10.1016/j.addr.2013.08.008.

[4] S. WANG, Y. MENG, C. LI, M. QIAN, and R. HUANG. Receptor-mediated drug delivery systems targeting to glioma. *Nanomaterials*. 2015, vol. 6, no. 1. Available from: https://doi.org/10.3390/nano6010003.

[5] J. V. GEORGIEVA, D. HOEKSTRA, and I. S. ZUHORN. Smuggling drugs into the brain: An overview of ligands targeting transcytosis for drug delivery across the blood–brain barrier. *Pharmaceutics*. 2014, vol. 6, no. 4, pp. 557–583. Available from: https://doi.org/10.3390/pharmaceutics6040557.

[6] W. M. PARDRIDGE. Molecular Trojan horses for blood-brain barrier drug delivery. *Curr. Opin. Pharmacol.* 2006, vol. 6, no. 5, pp. 494–500. Available from: https://doi.org/10.1016/j.coph.2006.06.001.

[7] M. AMIRI, M. SALAVATI-NIASARI, and A. AKBARI. Magnetic nanocarriers: Evolution of spinel ferrites for medical applications. *Adv. Colloid Interface Sci.* 2019, vol. 265, pp. 29–44. Available from: https://doi.org/10.1016/j.cis.2019.01.003.

[8] S. S. PATHAK *et al.* Magnetism in drug delivery: The marvels of iron oxides and substituted ferrites nanoparticles. *J. Magn. Magn. Mater.* 2021, vol. 12, no. 5, pp. 103–125. Available from: https://doi.org/10.1016/j.cis.2019.01.003.

[9] S. SHUKLA, P. K. DEHERI, and R. V. RAMANUJAN. Magnetic nanostructures: Synthesis, properties, and applications. In *Springer Handbook of Nanomaterials*. Springer Berlin Heidelberg, 2013, pp. 473–514.

[10] S. JAUHAR, J. KAUR, A. GOYAL, and S. SINGHAL. Tuning the properties of cobalt ferrite: a road towards diverse applications. *RSC Adv.* 2016, vol. 6, no. 100, pp. 97694–97719. Available from: https://doi.org/10.1039/C6RA21224G.

[11] C. TASSA, S. Y. SHAW, and R. WEISSLEDER. Dextran-coated iron oxide nanoparticles: A versatile platform for targeted molecular imaging, molecular diagnostics, and therapy. *Acc. Chem. Res.* 2011, vol. 44, no. 10, pp. 842–852. Available from: https://doi.org/10.1021/ar200084x.

[12] H. HERMAWAN, D. RAMDAN, and J. R. P. DJUANSJAH. World' s largest Science, Technology & Medicine Open Access book publisher Metals for Biomedical Applications. 2018, no. 2016, pp. 267–322.

[13] K. K. KEFENI, T. A. M. MSAGATI, and B. B. MAMBA. Ferrite nanoparticles: Synthesis, characterisation and applications in electronic device. *Materials Science and Engineering B: Solid-State Materials for Advanced Technology*. 2017. Available from: https://doi.org/10.1016/j.mseb.2016.11.002.

[14] M. W. MUSHTAQ *et al.* Synthesis and characterisation of doxorubicin-loaded functionalised cobalt ferrite nanoparticles and their in vitro anti-tumour activity under an AC-magnetic field. *Trop. J. Pharm. Res.*. 2017, vol. 16, no. 7, pp. 1663–1674. Available from: https://doi.org/10.4314/tjpr.v16i7.27.

[15] I. VITRO, S. MNGADI, S. MOKHOSI, and M. SINGH. Nanoparticles Enhance Delivery of 5-Fluorouracil. 2020.

[16] S. M. MNGADI, S. R. MOKHOSI, and M. SINGH. Surface-coating of Mg0.5Co0.5Fe2O4 nanoferrites and their in vitro cytotoxicity. *Inorg. Chem. Commun.* 2019, vol. 108, no. June, p. 107525. Available from: https://doi.org/10.1016/j.inoche.2019.107525.

[17] D. RAMNANDAN, S. MOKHOSI, A. DANIELS, and M. SINGH. Chitosan, polyethylene glycol and polyvinyl alcohol modified mgfe2 o4 ferrite magnetic nanoparticles in doxorubicin delivery: A comparative study in vitro. *Molecules*. 2021, vol. 26, no. 13. Available from: https://doi.org/10.3390/molecules26133893.

[18] B. OLLER-SALVIA, M. SÁNCHEZ-NAVARRO, E. GIRALT, and M. TEIXIDÓ. Blood–brain barrier shuttle peptides: an emerging paradigm for brain delivery. *Chem. Soc. Rev.* 2016, vol. 45, no. 17, pp. 4690–4707. Available from: https://doi.org/10.1039/C6CS00076B.

[19] Z. XU, Y. WANG, Z. MA, Z. WANG, Y. WEI, and X. JIA. A poly(amidoamine) dendrimer-based nanocarrier conjugated with Angiopep-2 for dual-targeting function in treating glioma cells. *Polym. Chem.* 2016, vol. 7, no. 3, pp. 715–721. Available from: https://doi.org/10.1039/c5py01625h.

[20] S. HABIB and M. SINGH. Angiopep-2-Modified Nanoparticles for Brain-Directed Delivery of Therapeutics: A Review. *Polymers (Basel).* 2022, vol. 14, no. 4. Available from: https://doi.org/10.3390/polym14040712.

[21] P. SONG, N. SONG, L. LI, M. WU, Z. LU, and X. ZHAO. Angiopep-2-Modified Carboxymethyl Chitosan-Based pH/Reduction Dual-Stimuli-Responsive Nanogels for Enhanced Targeting Glioblastoma. *Biomacromolecules*. 2021, vol. 22, no. 7, pp. 2921–2934. Available from: https://doi.org/10.1021/acs.biomac.1c00314.

[22] J. M. LAJOIE and E. V. SHUSTA. Targeting Receptor-Mediated Transport for Delivery of Biologics Across the Blood-Brain Barrier. *Annu. Rev. Pharmacol. Toxicol.* 2015, vol. 55, no. 1, pp. 613–631. Available from: https://doi.org/10.1146/annurev-pharmtox-010814-124852.

[23] Y. LI, X. ZHENG, M. GONG, and J. ZHANG. Delivery of a peptide-drug conjugate targeting the blood brain barrier improved the efficacy of paclitaxel against glioma. *Oncotarget*. 2016, vol. 7, no. 48, pp. 79401–79407. Available from: https://doi.org/10.18632/oncotarget.12708.

[24] W. B. DLAMINI, J. Z. MSOMI, and T. MOYO. XRD, Mössbauer and magnetic properties of MgxCo1-xFe2O4 nanoferrites. *J. Magn. Magn. Mater.* 2015, vol. 373, pp. 78–82. Available from: https://doi.org/10.1016/j.jmmm.2014.01.066.

[25] T. AZIZ, S. MASUM, M. QADIR, A. GAFUR, and D. HUQ. Physicochemical Characterization of Iron Oxide Nanoparticle Coated with Chitosan for Biomedical Application. *Int. Res. J. Pure Appl. Chem.* 2016, vol. 11, no. 1, pp. 1–9. Available from: https://doi.org/10.9734/irjpac/2016/23408.

[26] W. KE *et al.* Gene delivery targeted to the brain using an Angiopep-conjugated polyethyleneglycol-modified polyamidoamine dendrimer. *Biomaterials*. 2009, vol. 30, no. 36, pp. 6976–6985. Available from: https://doi.org/10.1016/j.biomaterials.2009.08.049.

[27] H. M. BERMAN *et al.*, “The protein data bank. *Acta Crystallogr. Sect. D Biol. Crystallogr.* 2002, vol. 58, no. 6 I, pp. 899–907. Available from: https://doi.org/10.1107/S0907444902003451.

[28] S. MNGADI, S. MOKHOSI, M. SINGH, and W. MDLALOSE. Chitosan-functionalized Mg0.5Co0.5Fe2O4 magnetic nanoparticles enhance delivery of 5-fluorouracil in vitro. *Coatings*. 2020, vol. 10, no. 5, pp. 1–13, Available from: https://doi.org/10.3390/COATINGS10050446.

[29] I. O. WULANDARI, H. SULISTYARTI, A. SAFITRI, D. J. D. H. SANTJOJO, and A. SABARUDIN. Development of synthesis method of magnetic nanoparticles modified by oleic acid and chitosan as a candidate for drug delivery agent. *J. Appl. Pharm. Sci.* 2019, vol. 9, no. 7, pp. 001–011. Available from: https://doi.org/10.7324/JAPS.2019.90701.

[30] W. B. MDLALOSE, S. DLAMINI, T. MOYO, S. R. MOKHOSI, and M. SINGH. Chitosan coating by mechanical milling of MnFe<inf>2</inf>O<inf>4</inf> and Mn<inf>0.5</inf>Co<inf>0.5</inf>Fe<inf>2</inf>O<inf>4</inf>: Effect of milling. In *Journal of Physics: Conference Series*. 2019, vol. 1310, no. 1. Available from: https://doi.org/10.1088/1742-6596/1310/1/012016.

[31] J. LI and C. SABLIOV. PLA/PLGA nanoparticles for delivery of drugs across the blood-brain barrier. *Nanotechnol. Rev.* 2013, vol. 2, no. 3, pp. 241–257. Available from: https://doi.org/10.1515/ntrev-2012-0084.

[32] Y. H. TSOU, X. Q. ZHANG, H. ZHU, S. SYED, and X. XU. Drug Delivery to the Brain across the Blood–Brain Barrier Using Nanomaterials. *Small*. 2017, vol. 13, no. 43, pp. 1–17. Available from: https://doi.org/10.1002/smll.201701921.

[33] S. R. MOKHOSI, W. MDLALOSE, S. MNGADI, M. SINGH, and T. MOYO. Assessing the structural, morphological and magnetic properties of polymer-coated magnesium-doped cobalt ferrite (CoFe2O4) nanoparticles for biomedical application. *J. Phys. Conf. Ser.* 2019, vol. 1310, no. 1, pp. 0–6. Available from: https://doi.org/10.1088/1742-6596/1310/1/012014.

[34] B. LIU *et al.* In-silico analysis of ligand-receptor binding patterns of α-MMC, TCS and MAP30 protein to LRP1 receptor. *J. Mol. Graph. Model.* 2020, vol. 98, p. 107619. Available from: https://doi.org/10.1016/j.jmgm.2020.107619.

[35] A. C. DI POLIDORO, A. CAFARCHIO, D. VECCHIONE, P. DONATO, F. DE NOLA, and E. TORINO. Revealing Angiopep-2/LRP1 Molecular Interaction for Optimal Delivery to Glioblastoma (GBM). *Molecules*. 2022, vol. 27, no. 19. Available from: https://doi.org/10.3390/molecules27196696.